Received: 17 January 2016 | Revised: 18 April 2016 | Accepted: 25 April 2016

DOI: 10.1111/cbdd.12787

RESEARCH ARTICLE

WILEY

PXD101 analogs with *L*-phenylglycine-containing branched cap as histone deacetylase inhibitors

Jingyao Li | Xiaoyang Li | Xue Wang | Jinning Hou | Jie Zang | Shuai Gao | Wenfang Xu | Yingjie Zhang

Department of Medicinal Chemistry, School of Pharmaceutical Sciences, Shandong University, Ji'nan, Shandong, China

Correspondence
Yingjie Zhang
Email: zhangyingjie@sdu.edu.cn

Histone deacetylases (HDACs) allow histones to wrap DNA more tightly and finally lead to the repression of some tumor suppressor genes. Histone deacetylase inhibitors (HDACIs) have been proved to have effects on tumorigenesis and tumor progression. In this study, we reported the design, synthesis, and *in vitro* activity evaluation of novel PXD101 analogs with *L*-phenylglycine-containing cap as HDACIs. Our results showed that HDACs inhibitory activities of compounds **10k**, **10r**, and **10s** were not only superior to the first approved HDACI SAHA, but also comparable to their parent compound PXD101, a recently approved HDACI in 2014. However, all 6 selected PXD101 analogs exhibited moderate *in vitro* antiproliferative activities, less potent than PXD101 and SAHA. Representative compound **10s** showed similar HDACs isoform selective profile to PXD101, which demonstrated that introduction of *L*-phenylglycine-containing branched cap group could not change the isoform selectivity of PXD101 dramatically.

KEYWORDS
antiproliferative activity, HDAC inhibitory activity, HDAC isoform selectivity, HDACs, inhibitor

Epigenetic abnormality, caused by different modifications of DNA and histones instead of changes of nucleotide sequence, has been recognized to be widely implicated in tumor initiation and progression, and their manipulation holds great promise for cancer prevention, detection, and therapy.[1] Histone deacetylases (HDACs), a histone modifier catalyzing the removal of acetyl groups from *N*-acetyl lysine residues of chromatin histones, allow histones to wrap DNA more tightly and finally lead to the repression of some tumor suppressor genes.[2,3]

So far, eighteen HDACs have been identified in humans, which have been classified in four classes depending on their sequence homology to the yeast original enzymes and domain organization.[4] The class I HDACs (HDAC1, 2, 3, and 8) are generally nuclear, while class II HDACs (IIa: HDAC4, 5, 7, and 9; IIb: HDAC6 and 10) can shuttle between the nucleus and the cytoplasm.[5,6] HDAC 11, the sole member of the class IV HDACs, is localized in both nucleus and cytoplasm.[7] The class III HDACs (SIRT1-7) are a set of NAD^+-dependent enzymes, while the other classes of HDACs are all Zn^{2+}-dependent enzymes which have been revealed to play a significant role in the process of tumorigenesis and development.[3] HDAC inhibitors (HDACIs) have been testified to cause tumor cell cycle arrest, apoptosis, cell differentiation, and migration suppression by blocking the act of HDACs.[8]

Up to now, dozens of structurally diverse HDACIs have entered various stages of clinical trials. Among them, 4 HDACIs have been approved by the US Food and Drug Administration (FDA) (Figure 1). Vorinostat (SAHA)[9] and

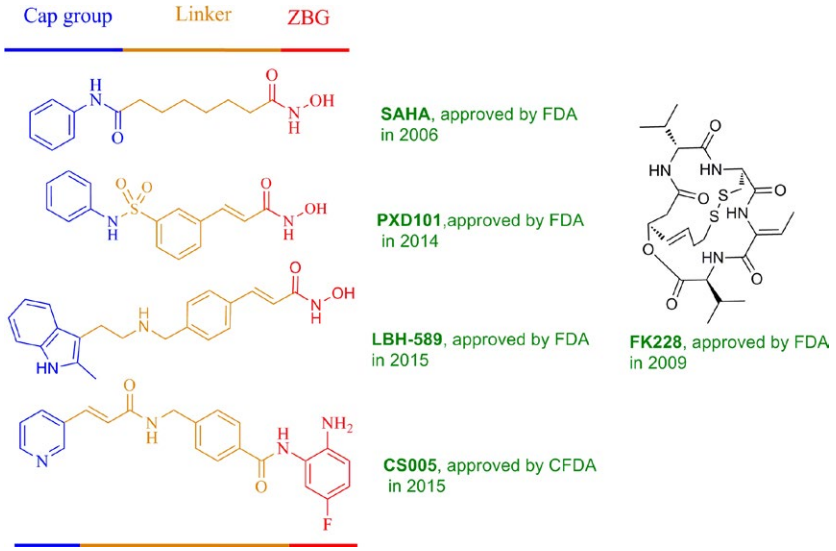

FIGURE 1 Pharmacophore model and structures of representative HDACIs

romidepsin (FK228)[10] were approved for the treatment of cutaneous T-cell lymphoma (CTCL), belinostat (PXD101)[11] was for the treatment of peripheral T-cell lymphoma (PTCL), and panobinostat (LBH589)[12] was for combination therapy of recurrent multiple myeloma with bortezomib and dexamethasone. In addition, the class I selective HDACI chidamide (CS005)[13] was approved by the China Food and Drug Administration (CFDA) for the treatment of relapsed or refractory PTCL.

PXD101 is a broad-acting HDACI which shows stability in diversified tumor types with low rates of adverse events, especially for the treatment of hematological malignancies indicated by a wide variety of clinical trials across a broad range of tumors.[11] Clinical researches of PXD101 for the treatment of ovary cancer, multiple myeloma, acute myeloid leukemia, and myelodysplastic syndrome as a single drug or combination drug therapy are still in progress. As most of the HDACIs, PXD101 has three pharmacophore domains, a Zn^{2+} binding group (ZBG), a hydrophobic cap group (Cap) and a linker which concatenate the ZBG and the cap group[14] (Figure 1).

Many researches indicated that HDACIs with branched cap seemed to be more potent and isoform selective due to the additional hydrophobic interactions between the branched cap group and the amino acid residues around the entrance of the HDAC active site.[15–20] In our previous study, two series of *L*-phenylglycine-containing cap HDAC inhibitors were discovered to have good performance in HDAC inhibition and antitumor evaluation.[21,22] Therefore, to find HDACI with improved potency and isoform selectivity, a novel series of PXD101 analogs were designed and synthesized by replacing the simple aniline-based cap group of PXD101 with *L*-phenylglycine-containing branched cap (Figure 2).

1 | METHODS AND MATERIALS

1.1 | Chemistry

All commercially available starting materials, reagents, and solvents were used without further purification unless otherwise stated. All reactions were monitored by TLC with 0.25 mm silica gel plates (60GF-254). UV light, iodine stain, and ferric chloride were used to visualize the spots. Silica gel was used for column chromatography purification. ^{1}H NMR and ^{13}C NMR spectra were recorded on a Bruker DRX spectrometer at 300, 400, or 600 MHz, *d* in parts per million and *J* in hertz, using TMS as an internal standard. High-resolution mass spectra were conducted by Shandong Analysis and Test Center in Ji'nan, China. ESI-MS spectra were recorded on an API 4000 spectrometer. Melting points were determined uncorrected on an electrothermal melting point apparatus.

The compound sodium 3-formylbenzenesulfonate (**2**) was synthesized following reported procedures.[23]

1.2 | General procedure for the preparation of 3

1.2.1 | Sodium (E)-3-(3-ethoxy-3-oxoprop-1-en-1-yl) benzenesulfonate (3)

A mixture of **2** (0.50 g, 2.40 mmol), K_2CO_3 (0.66 g, 4.80 mmol), triethyl phosphonoacetate (0.65 g, 2.88 mmol), and H_2O (5 mL) was stirred at room temperature for 30 min. Precipitated solid was filtered off and washed with MeOH. The filtrate was evaporated and dried to obtained product compound **3**, a pale

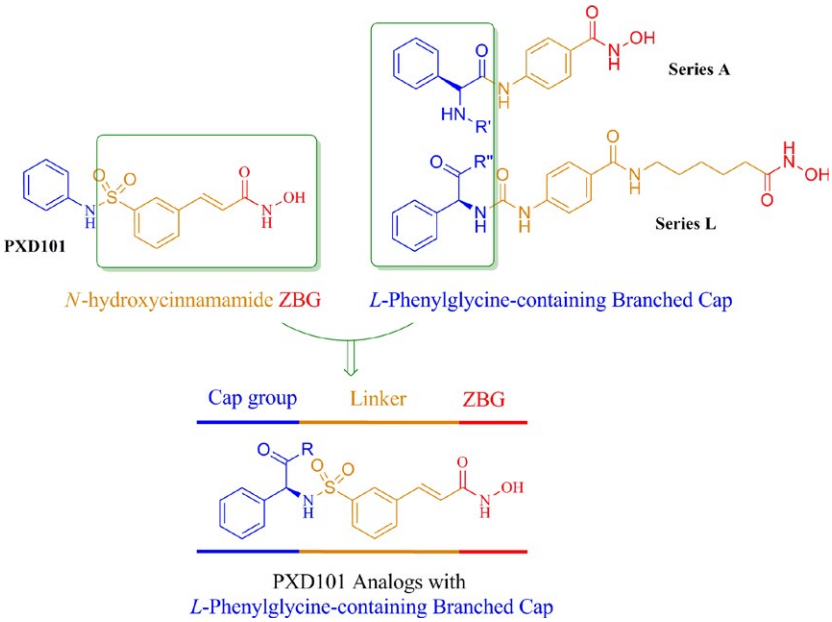

FIGURE 2 Design strategy of novel series of HDACIs

yellow oil (0.32 g, 48%), which was directly used for following reactions.

1.3 | General procedure for the preparation of 4

1.3.1 | (E)-ethyl 3-(3-(chlorosulfonyl) phenyl) acrylate (4)

A mixture of **3** (0.53 g, 2 mmol), $SOCl_2$ (1.70 mL, 13.8 mmol), and DMF (2 drops) was stirred under reflux for 5 h until the entire solid dissolved. The mixture was evaporated, and the yellow residue was directly used for following reactions.

The compound (*S*)-2-((tert-butoxycarbonyl) amino)-2-phenylacetic acid (**6**) was synthesized according to the methods described in our previous study.[21]

1.4 | General procedure for the preparation of 7a–7t

1.4.1 | (S)-tert-butyl (2-oxo-1-phenyl-2-(phenylamino) ethyl) carbamate (7a)

To a solution of compound **6** (1.26 g, 5 mmol) in DCM (50 mL), Et_3N (0.61 g, 6 mmol) and TBTU (1.93 g, 6 mmol) were added at 0 °C in turn. After 20 min, phenylamine (0.56 g, 6 mmol) was added in the mixture. The reaction was stirred at room temperature for 8 h. Then, the solvent was evaporated with the residue being taken up in EtOAc (100 mL). The EtOAc solution was washed with saturated citric acid (3 × 50 mL), $NaHCO_3$ (3 × 50 mL), and brine (3 × 50 mL); dried over $MgSO_4$ overnight; and evaporated under vacuum. The desired compound **7a** (1.44 g, 88% yield) was derived by crystallization in EtOAc as white powder. Mp: 116–118 °C ^{1}H NMR (300 MHz, DMSO-d_6) δ 10.25 (s, 1H), 7.61–7.44 (m, 5H), 7.33 (ddd, J = 19.3, 11.4, 4.7 Hz, 5H), 7.04 (t, J = 7.4 Hz, 1H), 5.36 (d, J = 8.3 Hz, 1H), 1.39 (s, 8H), 1.31 (s, 1H). ESI-MS: *m/z*: 327.2 $[M + H]^+$.

The other compounds (**7b–7t**) were prepared using the same procedure as described above.

1.5 | General procedure for the preparation of 8a–8t

1.5.1 | (S)-2-amino-*N*,2-diphenylacetamide hydrochloride (8a)

To a solution of compound **7a** (3.3 g, 10 mmol) in EtOAc (20 mL), a solution of EtOAc (40 mL) saturated by dry HCl gas was added. The reaction solution was stirred at room temperature for 5 h. Precipitates appeared and were filtered, with the filter being washed with ether, to give desired compound **8a** (1.94 g, 74% yield). Title compound was obtained as an amorphous white solid. Mp: 228–230 °C. ^{1}H NMR (400 MHz, DMSO-d_6) δ 11.25 (s, 1H), 8.94 (s, 3H), 7.71 (d, J = 6.9 Hz, 2H), 7.65 (d, J = 7.8 Hz, 2H), 7.49–7.39 (m, 3H), 7.32 (t, J = 7.9 Hz, 2H), 7.09 (t, J = 7.4 Hz, 1H), 5.33 (s, 1H). HRMS (AP-ESI) *m/z* calcd $[M + H]^+$ 227.1179.

The other compounds (**8b–8t**) were prepared using the same procedure as described above.

1.6 | General procedure for the preparation of 9a–9t

1.6.1 | (S,E)-ethyl3-(3-(*N*-(2-oxo-1-phenyl-2(phenylamino)ethyl)sulfamoyl)phenyl)acrylate (9a)

To a solution of compound **8a** (0.58 g, 2.2 mmol) in DCM (10 mL), Et_3N (0.24 g, 2.4 mmol), a solution of **4** (0.60 g, 2.2 mmol) in toluene (10 mL) was added in turn. The reaction solution was stirred at room temperature overnight. Then, the solvent was evaporated with the residue being taken up in EtOAc (60 mL). The EtOAc solution was washed with saturated citric acid (3 × 20 mL), $NaHCO_3$ (3 × 20 mL), and brine (3 × 20 mL); dried over $MgSO_4$; and evaporated under vacuum. The desired compound **9a** (0.82 g, 80% yield) was derived by crystallization in EtOAc as white powder. ^{1}H NMR (300 MHz, DMSO-d_6) δ 10.28 (s, 1H), 8.84 (d, J = 9.8 Hz, 1H), 8.00 (s, 1H), 7.76 (t, J = 8.0 Hz, 2H), 7.56–7.42 (m, 2H), 7.41 (d, J = 1.7 Hz, 1H), 7.38 (d, J = 1.3 Hz, 1H), 7.36 (d, J = 1.1 Hz, 1H), 7.33 (s, 1H), 7.30–7.15 (m, 5H), 7.00 (t, J = 7.3 Hz, 1H), 6.55 (d, J = 16.1 Hz, 1H), 5.25 (d, J = 9.8 Hz, 1H), 4.21 (q, J = 7.1 Hz, 2H), 1.28 (t, J = 7.1 Hz, 3H). ESI-MS: *m/z*: 465.3 $[M + H]^+$.

The other compounds (**9b–9t**) were prepared using the same procedure as described above.

1.7 | General procedure for the preparation of 10a–10t

1.7.1 | (S,E)-*N*-hydroxy-3-(3-(*N*-(2-oxo-1-phenyl-2-(phenylamino)ethyl)sulfamoyl)phenyl) acrylamide (10a)

Compound **9a** (0.46 g, 1.0 mmol) was dissolved in 14 mL of NH_2OK (0.17 g, 2.4 mmol) methanol solution and stirred for 3 h. After the reaction was complete, the solvent was evaporated under vacuum. The residue was acidified with saturated citric acid to a pH 3–4 and then extracted with EtOAc (3 × 20 mL). The organic layers were combined, washed with brine (3 × 20 mL), dried over $MgSO_4$, and evaporated under vacuum. The crude material was purified via flash chromatography to afford the desired compound **10a** (0.19 g, 42% yield) as pale yellow solid. Mp: 202–204 °C. ^{1}H NMR (600 MHz, DMSO-d_6) δ 10.89 (s, 1H), 10.38 (s, 1H), 10.27 (s, 2H), 8.86 (d, J = 9.6 Hz, 1H), 7.90 (s, 1H), 7.71 (d, J = 7.9 Hz, 1H), 7.60 (d, J = 7.7 Hz, 1H), 7.43–7.37 (m, 6H), 7.25–7.19 (m, 5H), 7.01 (t, J = 7.4 Hz, 1H), 6.51 (d, J = 15.8 Hz, 1H), 5.25 (d, J = 9.7 Hz, 1H). HRMS (AP-ESI) *m/z* calcd for $C_{23}H_{21}N_3O_5S$ $[M - H]^-$ 450.1131, found 450.1129.

1.7.2 | (S,E)-3-(3-(*N*-(2-(cyclohexylamino)-2-oxo-1-phenylethyl)sulfamoyl)phenyl)-*N*-hydroxyacrylamide (10b)

Pale yellow solid, 32% yield. Mp: 177–178 °C. ^{1}H NMR (300 MHz, DMSO-d_6) δ 10.85 (s, 1H), 9.10 (s, 1H), 8.59 (d, J = 8.6 Hz, 1H), 8.02 (d, J = 7.7 Hz, 1H), 7.86 (s, 1H), 7.76–7.64 (m, 2H), 7.47 (dd, J = 17.9, 11.7 Hz, 2H), 7.35–7.27 (m, 2H), 7.26–7.13 (m, 3H), 6.51 (d, J = 15.8 Hz, 1H), 5.01 (d, J = 8.4 Hz, 1H), 3.27–3.15 (m, 1H), 1.59–1.40 (m, 5H), 1.09–0.91 (m, 5H). HRMS (AP-ESI) *m/z* calcd for $C_{23}H_{27}N_3O_5S$ $[M - H]^-$ 456.1602, found 456.1599.

1.7.3 | (S,E)-*N*-hydroxy-3-(3-(*N*-(2-oxo-1-phenyl-2-(propylamino)ethyl)sulfamoyl)phenyl) acrylamide (10c)

Pale yellow solid, 32% yield. Mp: 172–174 °C. ^{1}H NMR (400 MHz, DMSO-d_6) δ 10.85 (s, 1H), 9.13 (s, 1H), 8.60 (s, 1H), 8.15 (t, J = 5.3 Hz, 1H), 7.85 (s, 1H), 7.69 (t, J = 7.6 Hz, 2H), 7.46 (dd, J = 20.3, 12.2 Hz, 2H), 7.30 (d, J = 6.9 Hz, 2H), 7.20 (dd, J = 15.6, 8.0 Hz, 3H), 6.50 (d, J = 15.8 Hz, 1H), 4.98 (d, J = 9.6 Hz, 1H), 2.85–2.68 (m, 2H), 1.28–1.12 (m, 3H), 0.66 (t, J = 7.4 Hz, 3H). HRMS (AP-ESI) *m/z* calcd for $C_{20}H_{23}N_3O_5S$ $[M - H]^-$ 416.1284, found 416.1286.

1.7.4 | (S,E)-*N*-hydroxy-3-(3-(*N*-(2-(isopropylamino)-2-oxo-1-phenylethyl)sulfamoyl) phenyl)acrylamide (10d)

Pale yellow solid, 27% yield. Mp: 174–175 °C. ^{1}H NMR (300 MHz, DMSO-d_6) δ 10.84 (s, 1H), 9.10 (s, 1H), 8.58 (d, J = 9.7 Hz, 1H), 8.02 (d, J = 7.4 Hz, 1H), 7.87 (s, 1H), 7.70 (dd, J = 8.1, 1.4 Hz, 2H), 7.53–7.40 (m, 2H), 7.30 (dd, J = 7.9, 1.5 Hz, 2H), 7.26–7.16 (m, 3H), 6.50 (d, J = 15.8 Hz, 1H), 4.96 (d, J = 9.7 Hz, 1H), 3.50 (dq, J = 13.3, 6.6 Hz, 1H), 0.83 (dd, J = 6.6, 1.6 Hz, 6H). HRMS (AP-ESI) *m/z* calcd for $C_{20}H_{23}N_3O_5S$ $[M - H]^-$ 416.1291, found 416.1286.

1.7.5 | (S,E)-3-(3-(*N*-(2-(butylamino)-2-oxo-1-phenylethyl)sulfamoyl)phenyl)-*N*-hydroxyacrylamide (10e)

Pale yellow solid, 29% yield. Mp: 178–179 °C. ^{1}H NMR (300 MHz, DMSO-d_6) δ 10.83 (s, 1H), 9.10 (s, 1H), 8.59 (d, J = 9.6 Hz, 1H), 8.11 (t, J = 5.4 Hz, 1H), 7.86 (s, 1H), 7.74–7.65 (m, 2H), 7.53–7.40 (m, 2H), 7.30 (dd, J = 7.9, 1.6 Hz, 2H), 7.26–7.16 (m, 3H), 6.50 (d, J = 15.8 Hz, 1H), 4.97 (d, J = 9.6 Hz, 1H), 2.90–2.70 (m, 2H), 1.20–0.98 (m, 4H), 0.75 (t, J = 7.1 Hz, 3H). HRMS (AP-ESI) *m/z* calcd for $C_{21}H_{25}N_3O_5S$ $[M - H]^-$ 430.1445, found 430.1442.

1.7.6 | (S,E)-*N*-hydroxy-3-(3-(N-(2-(isobutylamino)-2-oxo-1-phenylethyl)sulfamoyl)phenyl) acrylamide (10f)

Pale yellow solid, 25% yield. Mp: 174–176 °C. ^{1}H NMR (300 MHz, DMSO-d_6) δ 10.83 (s, 1H), 9.10 (d, J = 1.3 Hz, 1H), 8.59 (d, J = 9.6 Hz, 1H), 8.12 (t, J = 5.7 Hz, 1H), 7.85 (s, 1H), 7.73–7.65 (m, 2H), 7.52–7.39 (m, 2H), 7.31 (dd, J = 7.9, 1.5 Hz, 2H), 7.25–7.15 (m, 3H), 6.49 (d, J = 15.8 Hz, 1H), 5.02 (d, J = 9.5 Hz, 1H), 2.66 (t, J = 6.3 Hz, 2H), 1.45 (dp, J = 13.4, 6.8 Hz, 1H), 0.64 (d, J = 6.6 Hz, 6H). HRMS (AP-ESI) *m/z* calcd for $C_{21}H_{25}N_3O_5S$ [M − H]$^-$ 430.1446, found 430.1442.

1.7.7 | (S,E)-3-(3-(*N*-(2-(tert-butylamino)-2-oxo-1-phenylethyl)sulfamoyl)phenyl)-*N*-hydroxyacrylamide (10g)

Pale yellow solid, 28% yield. Mp: 182–184 °C. ^{1}H NMR (300 MHz, DMSO-d_6) δ 10.84 (s, 1H), 8.49 (d, J = 9.9 Hz, 1H), 7.91 (s, 1H), 7.75 (d, J = 4.7 Hz, 2H), 7.71 (d, J = 1.2 Hz, 1H), 7.57–7.46 (m, 2H), 7.44 (s, 1H), 7.32 (d, J = 6.7 Hz, 2H), 7.28–7.18 (m, 3H), 6.52 (d, J = 15.8 Hz, 1H), 5.03 (d, J = 9.8 Hz, 1H), 0.99 (s, 9H). HRMS (AP-ESI) *m/z* calcd for $C_{21}H_{25}N_3O_5S$ [M − H]$^-$ 430.1447, found 430.1442.

1.7.8 | (S,E)-3-(3-(*N*-(2-((4-fluorophenyl) amino)-2-oxo-1-phenylethyl)sulfamoyl)phenyl)-*N*-hydroxyacrylamide(10h)

Pale yellow solid, 27% yield. Mp: 130–132 °C. ^{1}H NMR (600 MHz, DMSO-d_6) δ 10.89 (s, 1H), 10.52 (s, 1H), 10.08 (s, 1H), 8.88 (d, J = 9.7 Hz, 1H), 7.90 (s, 1H), 7.71 (d, J = 7.9 Hz, 1H), 7.61 (d, J = 7.7 Hz, 1H), 7.44–7.36 (m, 6H), 7.25 (t, J = 7.3 Hz, 2H), 7.23–7.19 (m, 1H), 7.05 (t, J = 8.9 Hz, 2H), 6.52 (d, J = 15.8 Hz, 1H), 5.24 (d, J = 9.6 Hz, 1H). HRMS (AP-ESI) *m/z* calcd for $C_{23}H_{20}FN_3O_5S$ [M − H]$^-$ 468.1039, found 468.1035.

1.7.9 | (S,E)-3-(3-(*N*-(2-((4-chlorophenyl) amino)-2-oxo-1-phenylethyl)sulfamoyl)phenyl)-*N*-hydroxyacrylamide (10i)

Pale yellow solid, 24% yield. Mp: 204–206 °C. ^{1}H NMR (600 MHz, DMSO-d_6) δ 10.88 (s, 1H), 10.54 (s, 1H), 9.14 (s, 1H), 8.89 (s, 1H), 7.90 (s, 1H), 7.70 (d, J = 7.8 Hz, 1H), 7.61 (d, J = 7.8 Hz, 1H), 7.43–7.35 (m, 6H), 7.29–7.20 (m, 5H), 6.50 (d, J = 15.8 Hz, 1H), 5.23 (s, 1H). HRMS (AP-ESI) *m/z* calcd for $C_{23}H_{20}ClN_3O_5S$ [M − H]$^-$ 484.0738, found 484.0739.

1.7.10 | (S,E)-3-(3-(*N*-(2-((4-bromophenyl) amino)-2-oxo-1-phenylethyl)sulfamoyl)phenyl)-*N*-hydroxyacrylamide (10j)

Pale yellow solid, 31% yield. Mp: 223–225 °C. ^{1}H NMR (600 MHz, DMSO-d_6) δ 10.87 (s, 1H), 10.48 (s, 1H), 9.14 (s, 1H), 8.89 (d, J = 9.6 Hz, 1H), 7.89 (s, 1H), 7.70 (d, J = 7.8 Hz, 1H), 7.62 (d, J = 7.7 Hz, 1H), 7.39 (ddd, J = 22.9, 16.2, 8.4 Hz, 8H), 7.23 (dt, J = 24.3, 7.1 Hz, 3H), 6.49 (d, J = 15.8 Hz, 1H), 5.21 (d, J = 9.4 Hz, 1H). HRMS (AP-ESI) *m/z* calcd for $C_{23}H_{20}BrN_3O_5S$ [M − H]$^-$ 528.0235, found 528.0234.

1.7.11 | (S,E)-*N*-hydroxy-3-(3-(*N*-(2-((4-iodophenyl) amino)-2-oxo-1-phenylethyl)sulfamoyl) phenyl) acrylamide (10k)

Pale yellow solid, 26% yield. Mp: 200–202 °C. ^{1}H NMR (600 MHz, DMSO-d_6) δ 10.85 (s, 1H), 10.31 (d, J = 68.5 Hz, 1H), 9.14 (s, 1H), 8.86 (s, 1H), 7.89 (s, 1H), 7.69 (t, J = 7.8 Hz, 1H), 7.62 (t, J = 7.2 Hz, 1H), 7.57 (d, J = 8.7 Hz, 1H), 7.44–7.34 (m, 5H), 7.27–7.19 (m, 5H), 6.46 (dd, J = 15.8, 8.0 Hz, 1H), 5.20 (d, J = 16.7 Hz, 1H). HRMS (AP-ESI) *m/z* calcd for $C_{23}H_{20}IN_3O_5S$ [M − H]$^-$ 576.0101, found 576.0096.

1.7.12 | (S,E)-*N*-hydroxy-3-(3-(*N*-(2-((4-methoxyphenyl)amino)-2-oxo-1-phenylethyl) sulfamoyl) phenyl)acrylamide (10l)

Pale yellow solid, 23% yield. Mp: 197–199 °C. ^{1}H NMR (600 MHz, DMSO-d_6) δ 10.85 (s, 1H), 10.12 (s, 1H), 9.14 (s, 1H), 8.81 (d, J = 9.6 Hz, 1H), 7.88 (s, 1H), 7.70 (d, J = 7.9 Hz, 1H), 7.63 (d, J = 7.7 Hz, 1H), 7.45–7.33 (m, 4H), 7.25 (dd, J = 13.3, 8.3 Hz, 4H), 7.20 (t, J = 7.2 Hz, 1H), 6.80 (d, J = 9.0 Hz, 2H), 6.46 (d, J = 15.8 Hz, 1H), 5.17 (d, J = 9.6 Hz, 1H), 3.69 (s, 3H). HRMS (AP-ESI) *m/z* calcd for $C_{24}H_{23}N_3O_6S$ [M − H]$^-$ 480.1234, found 480.1235.

1.7.13 | (S,E)-*N*-hydroxy-3-(3-(*N*-(2-oxo-1-phenyl-2-(o-tolylamino)ethyl)sulfamoyl)phenyl) acrylamide (10m)

Pale yellow solid, 28% yield. Mp: 161–163 °C. ^{1}H NMR (600 MHz, DMSO-d_6) δ 10.86 (s, 1H), 9.65 (s, 1H), 9.14 (s, 1H), 8.85 (d, J = 9.6 Hz, 1H), 7.93 (s, 1H), 7.76 (d, J = 7.8 Hz, 1H), 7.71 (d, J = 7.5 Hz, 1H), 7.50 (t, J = 7.8 Hz, 1H), 7.44 (t, J = 12.3 Hz, 3H), 7.27 (t, J = 7.4 Hz, 2H), 7.23 (t, J = 7.2 Hz, 1H), 7.12 (d, J = 7.3 Hz, 1H), 7.09–7.01 (m, 2H), 6.99 (d, J = 7.7 Hz, 1H), 6.51 (d, J = 15.8 Hz, 1H), 5.33 (d, J = 9.5 Hz,

1H), 1.89 (s, 3H). HRMS (AP-ESI) *m/z* calcd for $C_{24}H_{23}N_3O_5S$ [M − H]$^-$ 464.1292, found 464.1286.

1.7.14 | (S,E)-3-(3-(*N*-(2-((2-chlorophenyl) amino)-2-oxo-1-phenylethyl)sulfamoyl)phenyl)-*N*-hydroxyacrylamide (10n)

Pale yellow solid, 25% yield. Mp: 158–160 °C. ^{1}H NMR (600 MHz, DMSO-d_6) δ 10.85 (s, 1H), 9.89 (s, 1H), 9.13 (s, 1H), 8.88 (s, 1H), 7.93 (s, 1H), 7.76 (d, J = 7.8 Hz, 1H), 7.71 (d, J = 7.9 Hz, 1H), 7.50 (t, J = 7.8 Hz, 1H), 7.46–7.37 (m, 4H), 7.26 (ddd, J = 14.0, 13.0, 5.3 Hz, 5H), 7.16 (t, J = 6.9 Hz, 1H), 6.50 (d, J = 15.8 Hz, 1H), 5.45 (s, 1H). HRMS (AP-ESI) *m/z* calcd for $C_{23}H_{20}ClN_3O_5S$ [M − H]$^-$ 484.0745, found 484.0739.

1.7.15 | (S,E)-3-(3-(*N*-(2-((3-fluorophenyl) amino)-2-oxo-1-phenylethyl)sulfamoyl)phenyl)-*N*-hydroxyacrylamide (10o)

Pale yellow solid, 22% yield. Mp: 204–205 °C. ^{1}H NMR (600 MHz, DMSO-d_6) δ 10.84 (s, 1H), 10.48 (s, 1H), 9.13 (s, 1H), 8.89 (s, 1H), 7.88 (s, 1H), 7.70 (d, J = 7.8 Hz, 1H), 7.62 (d, J = 7.6 Hz, 1H), 7.43 (t, J = 7.8 Hz, 1H), 7.40–7.35 (m, 3H), 7.33 (d, J = 11.5 Hz, 1H), 7.30–7.24 (m, 3H), 7.24–7.19 (m, 1H), 7.09 (d, J = 8.1 Hz, 1H), 6.86 (dd, J = 8.3, 6.4 Hz, 1H), 6.45 (d, J = 15.8 Hz, 1H), 5.19 (d, J = 4.6 Hz, 1H). HRMS (AP-ESI) *m/z* calcd for $C_{23}H_{20}FN_3O_5S$ [M − H]$^-$ 468.104, found 468.1035.

1.7.16 | (S,E)-*N*-hydroxy-3-(3-(*N*-(2-((3-methoxyphenyl)amino)-2-oxo-1-phenylethyl) sulfamoyl) phenyl)acrylamide (10p)

Pale yellow solid, 22% yield. Mp: 205–206 °C. ^{1}H NMR (600 MHz, DMSO-d_6) δ 10.84 (s, 1H), 10.24 (s, 1H), 9.13 (s, 1H), 8.85 (d, J = 9.5 Hz, 1H), 7.88 (s, 1H), 7.70 (d, J = 7.8 Hz, 1H), 7.62 (d, J = 7.7 Hz, 1H), 7.45–7.34 (m, 4H), 7.25 (t, J = 7.3 Hz, 2H), 7.20 (t, J = 7.2 Hz, 1H), 7.13 (t, J = 8.1 Hz, 1H), 7.05 (s, 1H), 6.92 (d, J = 8.0 Hz, 1H), 6.60 (dd, J = 8.2, 1.8 Hz, 1H), 6.46 (d, J = 15.8 Hz, 1H), 5.19 (d, J = 9.5 Hz, 1H), 3.68 (s, 3H). HRMS (AP-ESI) *m/z* calcd for $C_{24}H_{23}N_3O_6S$ [M − H]$^-$ 480.1242, found 480.1235.

1.7.17 | (S,E)-3-(3-(*N*-(2-((2-chlorophenethyl) amino)-2-oxo-1-phenylethyl)sulfamoyl) phenyl)-*N*-hydroxyacrylamide (10q)

Pale yellow solid, 30% yield. Mp: 122–124 °C. ^{1}H NMR (300 MHz, DMSO-d_6) δ 10.90 (s, 1H), 9.11 (s, 1H), 8.78 (d, J = 5.8 Hz, 1H), 8.71 (d, J = 9.3 Hz, 1H), 7.88 (s, 1H), 7.70 (d, J = 7.8 Hz, 2H), 7.47 (t, J = 7.8 Hz, 1H), 7.43–7.38 (m, 1H), 7.37 (d, J = 1.1 Hz, 1H), 7.35 (d, J = 2.1 Hz, 1H), 7.32 (d, J = 1.4 Hz, 1H), 7.24 (s, 1H), 7.23–7.18 (m, 3H), 7.14 (td, J = 7.5, 1.1 Hz, 1H), 6.92 (d, J = 7.5 Hz, 1H), 6.56 (d, J = 15.7 Hz, 1H), 5.13 (d, J = 9.4 Hz, 1H), 4.13 (d, J = 5.2 Hz, 2H). HRMS (AP-ESI) *m/z* calcd for $C_{25}H_{24}ClN_3O_5S$ [M − H]$^-$ 498.0901, found 498.0896.

1.7.18 | (S,E)-*N*-hydroxy-3-(3-(*N*-(2-oxo-2-(phenethylamino)-1-phenylethyl)sulfamoyl) phenyl) acrylamide (10r)

Pale yellow solid, 31% yield. Mp: 156–158 °C. ^{1}H NMR (600 MHz, DMSO-d_6) δ 10.85 (s, 1H), 9.14 (s, 1H), 8.62 (s, 1H), 8.28 (t, J = 5.4 Hz, 1H), 7.87 (s, 1H), 7.70 (dd, J = 13.6, 7.8 Hz, 2H), 7.49 (t, J = 7.8 Hz, 1H), 7.45 (d, J = 15.9 Hz, 1H), 7.26 (d, J = 6.5 Hz, 2H), 7.23–7.18 (m, 5H), 7.17–7.13 (m, 1H), 7.00 (d, J = 7.0 Hz, 2H), 6.52 (d, J = 15.8 Hz, 1H), 4.97 (s, 1H), 3.07 (td, J = 13.1, 7.1 Hz, 1H), 3.01 (td, J = 13.0, 7.2 Hz, 1H), 2.48 (t, J = 7.4 Hz, 2H). HRMS (AP-ESI) *m/z* calcd for $C_{25}H_{25}N_3O_5S$ [M − H]$^-$ 478.144, found 478.1442.

1.7.19 | (S,E)-*N*-hydroxy-3-(3-(*N*-(2-(naphthalen-1-ylamino)-2-oxo-1-phenylethyl)sulfamoyl)phenyl) acrylamide (10s)

Pale yellow solid, 26% yield. Mp: 186–188 °C. ^{1}H NMR (300 MHz, DMSO-d_6) δ 10.84 (s, 1H), 10.24 (s, 1H), 9.11 (s, 1H), 8.89 (d, J = 9.5 Hz, 1H), 7.98 (s, 1H), 7.89 (d, J = 7.7 Hz, 1H), 7.79 (d, J = 7.9 Hz, 1H), 7.72 (t, J = 7.7 Hz, 2H), 7.60 (d, J = 8.1 Hz, 1H), 7.49 (t, J = 7.5 Hz, 4H), 7.45–7.36 (m, 2H), 7.30 (dt, J = 11.7, 6.8 Hz, 4H), 6.52 (d, J = 15.8 Hz, 1H), 5.50 (d, J = 9.5 Hz, 1H). HRMS (AP-ESI) *m/z* calcd for $C_{27}H_{23}N_3O_5S$ [M − H]$^-$ 500.1289, found 500.1286.

1.7.20 | (S,E)-*N*-hydroxy-3-(3-(*N*-(2-((naphthalen-1-ylmethyl)amino)-2-oxo-1-phenylethyl)sulfamoyl)phenyl) acrylamide (10t)

Pale yellow solid, 24% yield. Mp: 158–160 °C. ^{1}H NMR (300 MHz, DMSO-d_6) δ 10.84 (s, 1H), 9.11 (s, 1H), 8.71 (t, J = 5.2 Hz, 2H), 7.91 (d, J = 7.6 Hz, 1H), 7.87 (s, 1H), 7.81 (d, J = 8.4 Hz, 2H), 7.68 (d, J = 7.8 Hz, 2H), 7.54 – 7.38 (m, 4H), 7.38–7.26 (m, 3H), 7.24–7.11 (m, 4H), 6.51 (d, J = 15.8 Hz, 1H), 5.10 (d, J = 8.4 Hz, 1H), 4.53 (qd, J = 15.2, 5.5 Hz, 2H). HRMS (AP-ESI) *m/z* calcd for $C_{28}H_{25}N_3O_5S$ [M − H]$^-$ 514.1443, found 514.1442.

1.8 | *In vitro* HDACs inhibition fluorescence assay

In vitro HDACs inhibition assays were conducted as previously described in our group.[24] In brief, 10 μL of enzyme solution (HeLa nuclear extracts, HDAC1, HDAC4, HDAC6, HDAC8, HDAC11) was mixed with various concentrations of target compounds (50 μL), SAHA, and PXD101, using 100% and none HDACs groups as control group. After incubation at 37 °C for 10 min, 40 μL of fluorogenic substrate (Boc-Lys(Ac)-AMC for HeLa nuclear extracts; Ac-Leu-GlyLyS(Ac)-AMC for HDAC1, HDAC6, and HDAC11; Ac-Leu-GlyLyS(Tfa)-AMC for HDAC4 and HDAC8) was added, and then, the mixture was incubated at 37 °C for 30 min. The mixture was stopped by addition of 100 μL of developer containing trypsin and TSA afterward. Over the next incubation at 37 °C for 20 min, fluorescence intensity was measured using a microplate reader at excitation and emission wavelengths of 390 and 460 nm, respectively. The inhibition ratios were calculated from the fluorescence intensity readings of tested wells relative to those of control wells, and the IC_{50} values were calculated using a regression analysis of the concentration/inhibition data.

1.9 | *In vitro* antiproliferative assay

In vitro antiproliferative assays were determined by the MTT (3-(4,5-dimethylthiazol-2-yl)-2,5-diphenyltetrazolium bromide) method as previously described. Briefly, all cell lines were maintained in RPMI1640 medium containing 10% FBS at 37 °C in 5% CO_2 humidified incubator. Cell proliferation assay was determined by the MTT method. Cells were passaged the day before dosing into a 96-well cell plate and allowed to grow for 12 h ahead of addition of tested compounds. These tested compounds were all dissolved in DMSO and then diluted in culture medium maintaining the effective DMSO concentration <0.2%. The plates were incubated for an additional 48 h afterward, and then, a 0.5% MTT solution was added to each well. After incubation for another 4 h, formazan formed from MTT was extracted by adding 200 μL of DMSO for 15 min. Absorbance was then determined using an ELISA reader at 570 nm.

1.10 | Molecular docking studies

Compounds were docked into the active site of HDAC2 (PDB entry: 4LXZ) using Tripos SYBYL X 2.0 (Certara USA, Inc., Princeton, NJ, USA). Before the docking process, the protein structure was treated by deleting water molecules, adding hydrogen atoms, fixing atom types, and assigning AMBER7 FF99 charges. A 100-step minimization process was performed to further optimize the protein structure. The molecular structures were generated with the Sybyl/Sketch module and optimized using Powell's method with the Tripos force field with convergence criterion set at 0.05 kcal/(Å mol) and assigned charges with the Gasteiger-Hückel method. Molecular docking was carried out *via* the Sybyl/FlexX module. Other docking parameters were kept to the default values.

2 | RESULTS AND DISCUSSION

2.1 | Chemistry

The target compounds **10a–10t** were synthesized following the procedures described in Scheme 1. Sulfonation

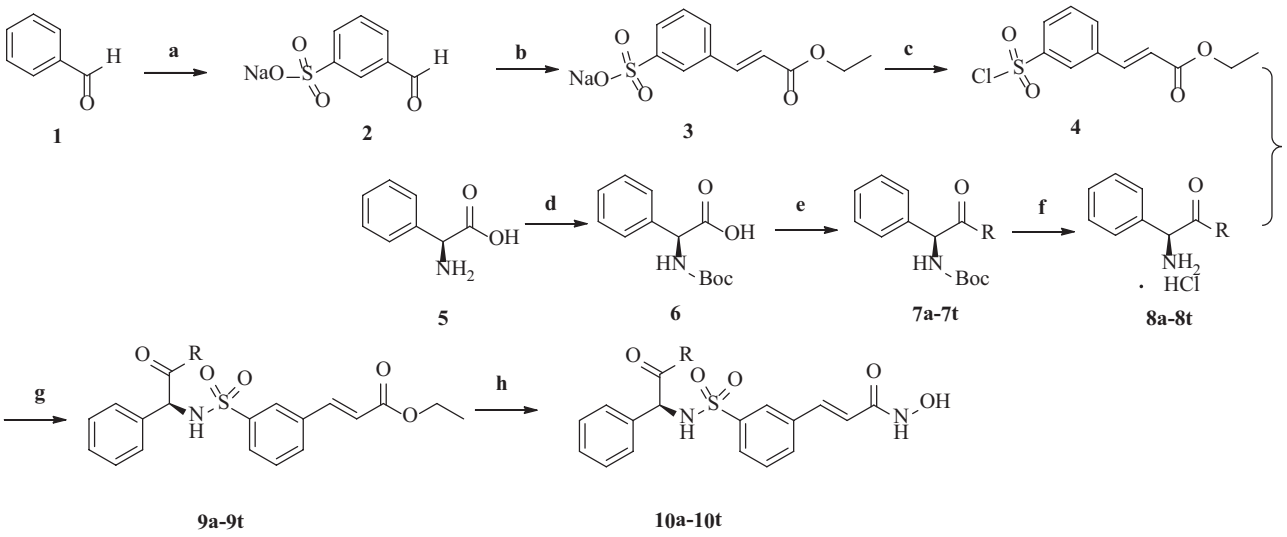

SCHEME 1 Synthesis of target compounds 10a-10t. Reagents and conditions: (a) Oleum, 40 °C 10 h, room temperature overnight; (b) triethyl phosphonoacetate, K_2CO_3, H_2O; (c) $SOCl_2$, DMF, 75 °C; (d) $(Boc)_2O$, Et_3N, $MeOH/H_2O$; (e) TBTU, Et_3N, THF; (f) HCl, anhydrous EtOAc; (g) PhMe; (h) NH_2OK, anhydrous MeOH

TABLE 1 HDAC inhibitory activity of compounds **10a–10t**

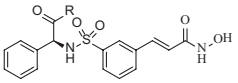

Compound	R	IC_{50} of HeLa extract[a] (nM)	Compound	R	IC_{50} of HeLa extract[a] (nM)
10a		136 ± 4	**10l**	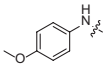	114 ± 1
10b		327 ± 13	**10m**		125 ± 9
10c		238 ± 13	**10n**		126 ± 9
10d		318 ± 1	**10o**		133 ± 6
10e		166 ± 5	**10p**		178 ± 7
10f		269 ± 2	**10q**		159 ± 8
10g		428 ± 17	**10r**	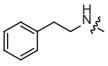	83 ± 1
10h		281 ± 10	**10s**		88 ± 1
10i	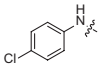	129 ± 2	**10t**		101 ± 5
10j	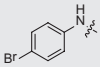	109 ± 3	SAHA		114 ± 1
10k		57 ± 1	PXD101		51 ± 2

[a]Assays were performed in replicate ($n \geq 2$); values are shown as mean ± SD.

of the starting material benzaldehyde (compound **1**) with oleum gave compound **2**. Under Horner–Wadsworth–Emmons reaction, compound **2** was converted to **3**, which was treated with thionyl chloride to get sulfonyl chlorides **4**. Boc (*tert*-butoxycarbonyl) group protection of another starting material *L*-phenylglycine (compound **5**) led to compound **6**, which reacted with appropriately various amines by TBTU-mediated amide formation to afford compound **7**. Subsequent *N*-deprotection of **7** afforded compound **8**. Compound **9** was prepared by coupling **4** with **8** and then treated with NH_2OK in methanol to give corresponding hydroxamic acids **10**.

2.2 | HeLa cell extract inhibitory assay by the target compounds

To efficiently screen our synthesized compounds with different hydrophobic substituents in the phenylglycine group of the cap, we conducted the enzymatic inhibitory assay against HeLa cell nuclear extracts (primarily containing HDAC1 and HDAC2) using SAHA and PXD101 as positive controls (Table 1). We first synthesized compounds (**10a–g**) substituted by phenylamine (**10a**) and various aliphatic amines (**10b–10g**) to figure out the disparate effects of aromatic and aliphatic substituents. Results indicated that **10a** with aromatic substituent was more potent than **10b–10g** with various aliphatic substituents.

For the purpose of probing effects of diverse substituents in the benzene ring of the R group in **10a**, we synthesized compounds with various *para*-substituent (**10h–l**), *ortho*-substituent (**10m–n**) and *meta*-substituent (**10o–p**). Results listed in Table 1 showed that most *para*-substituted derivatives except **10h** exhibited better HDAC inhibitory activities than **10a**. For *para*-substituted derivatives **10h–10k**, their inhibitory potency increased when the electron-withdrawing abilities of the substituent decreased, the most potent compound **10k** was superior to SAHA and comparable to PXD101. Compounds with *ortho*-substituent or *meta*-substituent displayed comparable inhibitory potency with **10a**, which indicated *ortho*-substituent or *meta*-substituent had no obvious effect on their HDAC inhibitory activities.

Moreover, compounds with phenylethyl substituent (**10r**), 1-naphthyl substituent (**10s**), and 1-menaphthyl substituent (**10t**) were synthesized to investigate the influence of volume and length of R group on HDACs inhibition. Results showed that **10r** and **10s** displayed better potency than SAHA.

2.3 | *In vitro* antiproliferative assay by the target compounds

For further investigation of the antiproliferative efficiency of our novel compounds, we first tested the inhibitory rate of all synthesized compounds at 5 μM against two human leukemia cell lines (U937 and HEL).[25] According to the preliminary results in Table 2, six compounds with relatively higher inhibition (**10k**, **10m**, **10o**, **10r**, **10s**, **10t**) were selected for further antiproliferative evaluation against 5 types of hematological tumor cell lines (Table 3). It was very disappointing that the overall antiproliferative activity of selected compounds was less potent than the positive control SAHA and PXD101 despite their better performance in the enzymatic inhibition assay.

TABLE 2 *In vitro* antiproliferative activity of compounds in U937 and HEL cell line

Compoundd	U937 (inhib%)[a,b]	HEL (inhib%)[a,b]	Compound	U937 (inhib%)[a,b]	HEL (inhib%)[a,b]
10a	48	18	**10l**	48	13
10b	42	11	**10m**	51	19
10c	10	12	**10n**	43	17
10d	14	13	**10o**	58	18
10e	38	15	**10p**	37	10
10f	41	14	**10q**	17	13
10g	23	9	**10r**	50	18
10h	36	10	**10s**	49	14
10i	44	14	**10t**	49	13
10j	47	18	SAHA	58	17
10k	48	20	PXD101	73	23

[a]Assays were performed in replicate ($n \geq 2$); the SD values are <20% of the mean.
[b]The activity was described as inhibition% at the concentration of 5 μM.

TABLE 3 *In vitro* antiproliferative activity of **10k**, **10m**, **10o**, **10r**, **10s**, and **10t**

	IC_{50}[a] (μM)				
Compound	HL60	U937	KG1	K562	U266
10k	2.1 ± 0.4	4.6 ± 0.1	5.0 ± 0.2	5.9 ± 0.1	6.1 ± 0.1
10m	2.6 ± 0.1	2.9 ± 0.1	4.2 ± 0.3	5.5 ± 0.1	5.6 ± 0.1
10o	4.0 ± 0.2	4.8 ± 0.4	5.0 ± 0.2	7.4 ± 0.2	6.3 ± 0.2
10r	3.9 ± 0.1	4.8 ± 0.5	5.1 ± 0.1	5.7 ± 0.1	5.9 ± 0.9
10s	2.5 ± 0.2	7.5 ± 0.1	4.8 ± 0.1	6.0 ± 0.6	5.6 ± 0.2
10t	4.9 ± 0.1	6.9 ± 1.4	4.4 ± 0.3	7.1 ± 0.1	5.8 ± 0.9
SAHA	0.8 ± 0.1	1.2 ± 0.1	1.4 ± 0.1	1.6 ± 0.1	0.7 ± 0.2
PXD101	0.2 ± 0.1	0.6 ± 0.1	0.8 ± 0.1	0.7 ± 0.1	0.7 ± 0.3

[a]Assays were performed in replicate ($n \geq 2$); values are shown as mean ± SD.

2.4 | HDAC isoform selectivity of 10s

To explore the HDAC isoform selectivity profile of these PXD101 analogs, the IC_{50} values of compound **10s** for class I representatives HDAC1 and HDAC8, class IIa representative HDAC4, class IIb representative HDAC6, and class IV isoform HDAC11 were determined with PXD101 as positive control (Table 4). Results presented in Table 4 demonstrated that **10s** exhibited similar overall selectivity profile with PXD101.

2.5 | Docking study

The proposed binding modes of compounds **10a** and **10b** (Figure 3) in the active site of HDAC2 (PDB code 4LXZ) were investigated by docking analysis. Figure 3A,B revealed that benzene ring of the external motif of **10a** could be well accommodated in the S' pocket of HDAC2, while cyclohexyl group of **10b** could hardly achieve the same effect. Moreover, chelation geometry of catalytic zinc ion demonstrated that although their hydroxamic acid group both chelated the zinc ion, **10a** (Figure 3C) displayed bidentate chelation with shorter measured distance between carbonyl and hydroxyl oxygens of hydroxamate and zinc ion, while **10b** (Figure 3D) exhibited weaker monodentate chelation. Furthermore, the H-bond interactions were detected in **10a** (Figure 3C) and **10b** (Figure 3D) for enhancing the ligand–receptor binding. The hydroxyl and carbonyl oxygens of **10a** have three H-bond interactions with His145, His146, and Tyr308, respectively, while only two H-bong interactions of **10b** with His145 and Gly154 were found. All the above information could rationalize the inhibitory activity of **10a** than **10b**.

TABLE 4 *In vitro* inhibition of HDACs isoforms of **10s**[a]

HDAC	IC_{50}[a] (nM)	
	10s	**PXD101**
Class I		
HDAC 1	93 ± 3	34 ± 4
HDAC 8	659 ± 50	353 ± 49
Class IIa		
HDAC 4	23 000 ± 2828	9850 ± 212
Class IIb		
HDAC 6	80 ± 17	27 ± 2
Class IV		
HDAC11	3850 ± 212	25 000 ± 8485

[a]Assays were performed in replicate ($n \geq 2$); values are shown as mean ± SD.

3 | CONCLUSION

In this article, we described the design, synthesis, and *in vitro* activity evaluation of a series of novel PXD101 analogs with *L*-phenylglycine-containing cap as HDACIs. Although *in vitro* HeLa cell extract inhibitory fluorescence assay showed that compounds **10k**, **10r**, and **10s** displayed potent HDAC inhibitory activity compared with approved drugs SAHA and PXD101, their antiproliferative potency was disappointing. **10s**, one of the most potent compounds, exhibited comparable similar overall isoform selective profile with PXD101. Collectively, our results showed that introduction of *L*-phenylglycine-containing branched cap group to PXD101 could not lead to analogs with improved potency or selectivity.

ACKNOWLEDGMENTS

This work was supported by National High-Tech R&D Program of China (863 Program) (Grant No. 2014AA020523), National Natural Science Foundation of China (Grant Nos. 21302111, 81373282, 21172134), China Postdoctoral Science Foundation funded project (Grant Nos. 2013M540558 and 2014T70654), Major Project of Science and Technology of Shandong Province

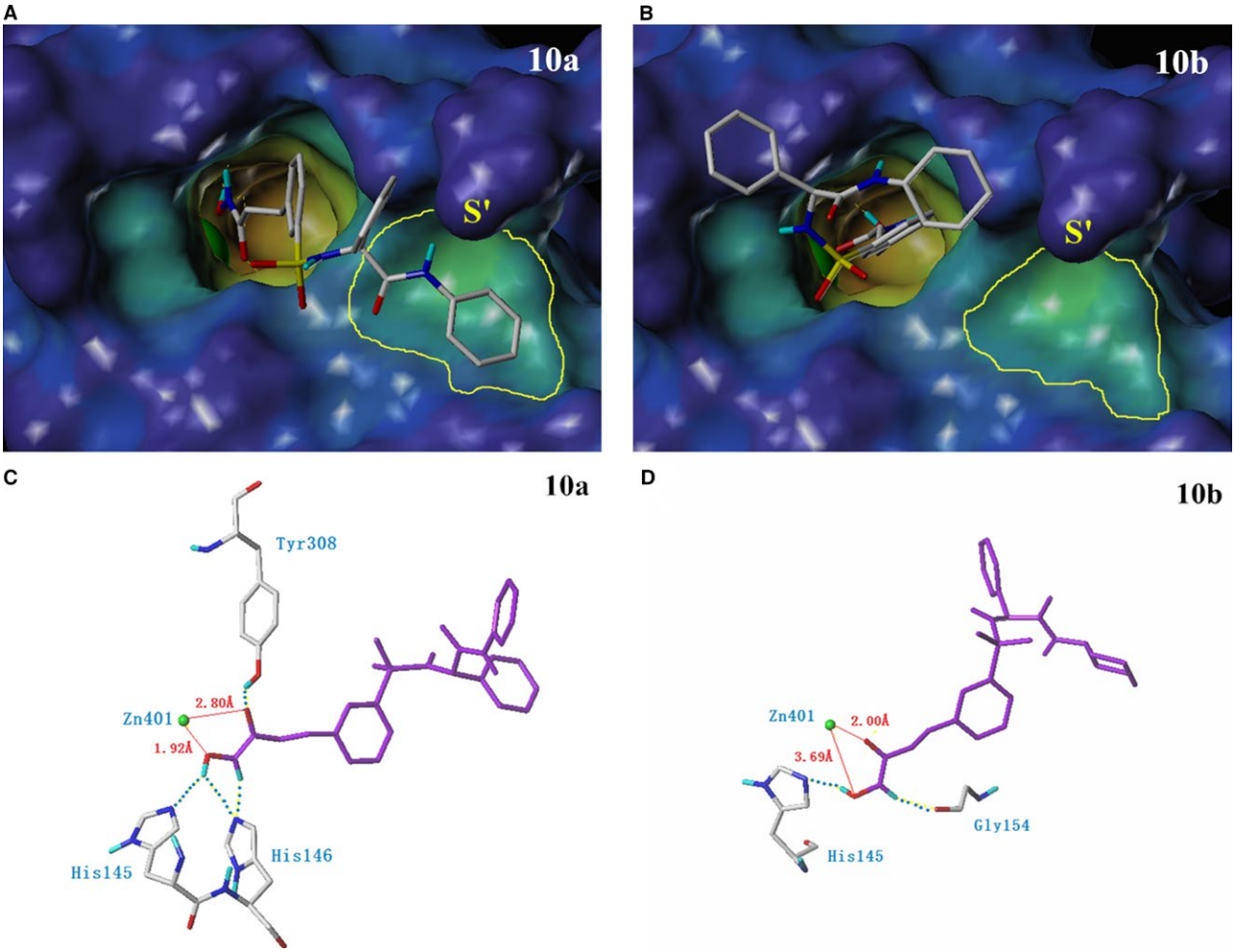

FIGURE 3 Proposed binding mode of compounds **10a** (A, C), **10b** (B, D) with HDAC2 (derived by modification of PDB code 4LXZ using Tripos SYBYL X 2.0). The zinc ion is shown as a green sphere. The H-bond is shown as dotted blue line (atom types: H, white; N, blue; O, red; S, yellow)

(2015ZDJS04001), Young Scholars Program of Shandong University (YSPSDU).

CONFLICT OF INTEREST

The authors confirm that this article content has no conflict of interest.

ABBREVIATIONS

CTCL, cutaneous T-cell lymphoma HDACIs, histone deacetylase inhibitors HDACs, histone deacetylases PTCL, peripheral T-cell lymphoma ZBG, zinc binding group.

REFERENCES

[1] K. Banno, I. Kisu, M. Yanokura, K. Tsuji, K. Masuda, A. Ueki, Y. Kobayashi, W. Yamagami, H. Nomura, E. Tominaga, N. Susumu, D. Aoki, *Int. J. Oncol.* **2012**, *41*, 793.
[2] J. G. Herman, S. B. Baylin, *N. Engl. J. Med.* **2003**, *349*, 2042.
[3] Y. Zhang, H. Fang, J. Jiao, W. Xu, *Curr. Med. Chem.* **2008**, *15*, 2840.
[4] M. Dokmanovic, C. Clarke, P. A. Marks, *Mol. Cancer Res.* **2007**, *5*, 981.
[5] S. A. M. Thiagalingam, K. H. Cheng, H. J. Lee, N. Mineva, N. Thiagalingam, J. F. Ponte, *Ann. N. Y. Acad. Sci.* 2003, 983(1), 84.
[6] H. L. Fitzsimons, *Neurobiol. Learn. Mem.* **2015**, *123*, 149.
[7] L. Gao, M. A. Cueto, F. Asselbergs, P. Atadja, *J. Biol. Chem.* **2002**, *277*, 25748.
[8] P. A. Marks, R. A. Rifkind, V. M. Richon, R. Breslow, T. Miller, W. K. Kelly, *Nat. Rev. Cancer* **2001**, *1*, 194.
[9] S. Grant, C. Easley, P. Kirkpatrick, *Nat. Rev. Drug Discov.* **2007**, *6*(1), 21.
[10] C. Campas-Moya, *Drugs Today* **2009**, *45*, 787.
[11] J. McDermott, A. Jimeno, *Drugs Today* **2014**, *50*, 337.
[12] H. M. Prince, M. J. Bishton, R. W. Johnstone, *Fut. Oncol.* **2009**, *5*, 601.
[13] B. Zhao, T. He, *Oncol. Rep.* **2015**, *33*(1), 304.
[14] E. Pontiki, D. Hadjipavlou-Litina, *Med. Res. Rev.* **2012**, *32*(1), 1.
[15] H. Su, L. Altucci, Q. You, *Mol. Cancer Ther.* **2008**, *7*, 1007.
[16] Y. Zhang, J. Feng, Y. Jia, Y. Xua, C. Liu, H. Fang, W. Xu, *Eur. J. Med. Chem.* **2011**, *46*, 5387.
[17] H. Su, L. Yu, A. Nebbioso, V. Carafa, Y. Chen, L. Altucci, Q. You, *Bioorg. Med. Chem. Lett.* **2009**, *19*, 6284.
[18] H. Rajak, A. Singh, K. Raghuwanshi, R. Kumar, P. K. Dewangan, R. Veerasamy, P. C. Sharma, A. Dixit, P. Mishra, *Curr. Med. Chem.* **2014**, *21*, 2642.
[19] M. S. Finnin, J. R. Donigian, A. Cohen, V. M. Richon, R. A. Rifkind, P. A. Marks, R. Breslow, N. P. Pavletich, *Nature* **1999**, *401*, 188.
[20] S. C. Mwakwari, W. Guerrant, V. Patil, S. I. Khan, B. L. Tekwani, A. Gurard-LevinZ, M. Mrksich, A. K. Oyelere, *J. Med. Chem.* **2010**, *53*, 6100.
[21] Y. Zhang, X. Li, J. Hou, Y. Huang, W. Xu, *Drug Des. Devel. Ther.* **2015**, *9*, 5553.
[22] L. Zhang, X. Wang, X. Li, X. Li, L. Zhang, W. Xu, *J. Enzyme Inhib. Med. Chem.* **2014**, *29*, 582.
[23] P. W. Finn, M. Bandara, C. Butcher, A. Finn, R. Hollinshead, N. Khan, N. Law, S. Murthy, R. Romero, C. Watkins, V. Andrianov, R. M. Bokaldere, K. Dikovska, V. Gailite, E. Loza, I. Piskunova, I. Starchenkov, M. Vorona, I. Kalvinsh, *Helv. Chim. Acta* **2005**, *88*, 1630.
[24] Y. Zhang, J. Feng, C. Liu, L. Zhang, J. Jiao, H. Fang, L. Su, X. Zhang, J. Zhang, M. Li, B. Wang, W. Xu, *Bioorg. Med. Chem.* **2010**, *18*, 1761.
[25] X. Li, E. S. Inks, X. Li, J. Hou, C. J. Chou, J. Zhang, Y. Jiang, Y. Zhang, W. Xu, *J. Med. Chem.* **2014**, *57*, 3324.